



1 **Assessment of Glacier Area Change in the Tekes River Basin, Central Tien Shan,**
2 **Kazakhstan Between 1976 and 2013 Using Landsat and KH-9 Imagery**

3

4 Zamira Usmanova ^{1,2,3}, Maria Shahgedanova ³, Igor Severskiy ¹, Gennady Nosenko ⁴, Vassiliy
5 Kapitsa ¹

6 ¹ Institute of Geography, Almaty, 050010, Kazakhstan;

7 ² al-Farabi Kazakh National University, Almaty, 050040, Kazakhstan;

8 ³ Department of Geography and Environmental Science and Walker Institute for Climate System
9 Research, University of Reading, Whiteknights, Reading RG6 6AB, UK;

10 ⁴ Laboratory of Glaciology, Institute of Geography of the Russian Academy of Sciences, 29
11 Staromonetny Pereulok, Moscow, 119017, Russia.

12 *Correspondence to:* Z. Usmanova (zamira_usmanova@mail.ru)

13

14 **Abstract**

15 Changes in glacierized area in the Kazakhstani sector of the Tekes River basin were assessed
16 using Landsat and KH-9 imagery from 2013, 1992 and 1976. Between 1992 and 2013, the
17 combined area of 118 glaciers declined from 121.4±9.2 km² to 105.0±5.5 km². The total area
18 loss was 16.4±5.9 km² or 13.5±7.5%. The rate of area reduction was 0.78 km² a⁻¹ or 0.64% a⁻¹.

19 This rate is lower than in other regions of northern Tien Shan because of the presence of several
20 large glaciers in the sample. The combined glacier area in 2013 exceeds the combined glacier
21 area reported by the RGI5.0 / GAMDAM inventories for 1999-2003 by 24% because the latter
22 did not include glacierized areas on slopes exceeding 40° and a number of small glaciers.

23 Changes in the recession rates between 1976, 1992 and 2013 were examined using a sub-sample
24 of 28 glaciers which occupied 61% of the total glacierized area in 1992 and 64 % in 2013. These
25 glaciers lost 8.3±5.6% in the 1976-1992 period, 8.4±5.9% in the 1992-2013 period and
26 16.0±5.8% between 1976 and 2013. The recession rates were 0.52±0.35% a⁻¹ in 1976-1992 and



27 $0.40 \pm 0.28\% \text{ a}^{-1}$ in 1992-2013 and although they appear to indicate a slow down in the glacier
28 recession, the change in the retreat rates is within the uncertainty of measurement. The relative
29 reduction in glacier area in the sub-sample is lower than for the basin as a whole because of a
30 larger size of glaciers. Temperature increase was observed in all seasons reaching 0.18°C per 10
31 years in summer and 0.39°C per 10 years in autumn in the 1947-2015 period. Precipitation
32 exhibited strong variability declining between 1952 and 1977 and then increasing until 2000s
33 with a number of dry years in the 2010s. There was no statistically significant difference
34 between the means of annual precipitation in the 1952-1977 and 1977-2015 periods. Combined
35 with the nearly steady recession rates, this suggests that it is an increase in summer, late spring
36 and early autumn temperature that drives glacier retreat.

37

38 **1 Introduction**

39 The Tien Shan mountains are one of the main centres of contemporary glaciation in Eurasia
40 where at present glaciers occupy, according to different estimates, between $15,416 \text{ km}^2$ to $16,427$
41 km^2 (Sorg et al., 2012). Glacier shrinkage has been observed in the region since the end of the
42 Little Ice Age (Solomina et al., 2004; Kutuzov and Shahgedanova, 2009) and recent assessments
43 suggest that overall, the Tien Shan lost $18 \pm 6\%$ and $27 \pm 15\%$ of glacierized area and mass
44 respectively between 1961 and 2012 (Farinotti et al., 2015). The rates of glacier recession vary
45 temporally and spatially because of complex topography, regional climatic differences and
46 variability in characteristics of glaciers potentially leading to variability in impacts of glacier
47 retreat such as changes in runoff and formation of glacier lakes. Table A1 presents glacier
48 recession rates as documented in the published literature illustrating both geographical and
49 temporal differences. The high retreat rates were observed in the southern Djungarskiy Alatau
50 and in Zailiyskiy Alatau (Solomina et al., 2004; Severskiy et al., 2016). At higher elevations in
51 the inner regions of the Tien Shan, glacier recession was slower. In the Saryjaz Ridge, the values
52 of glacier area change between 1990 and 2010 were close to the accuracy of measurements



53 (Osmonov et al., 2013). Pieczonka and Bolch (2015) reported similarly low recession rates for
54 the Kokshal-Too, Tomur and Inylchek regions and the Aksu catchment for the 1975-2008 period
55 as did Shannugan et al. (2009) for the Tarim basin in the Chinese Tien Shan by for the 1960s –
56 2000 period.

57 Most studies assess changes in the glacier extent for a single period (Table 1A). However, a
58 number of studies examining changes in recession rates over time highlight the acceleration of
59 glacier retreat in the last three decades, e.g. Aizen et al. (2006; 2007) in the Ala-Archa region
60 and Kutuzov and Shahgedanova (2009) in the Terskey-Alatoo. Having analysed Landsat, Corona
61 KH-4B and Hexagon KH-9 imagery, Narama et. al. (2010) reported a small acceleration of
62 glacier retreat in the western (Pskem) and northern (Ili – Kungey) Tien-Shan in the 2000-2007
63 period in comparison with the 1970-2000 period although it is not clear whether the reported
64 increase in the recession rates exceeds the uncertainty of measurements. By contrast, Severskiy
65 et al. (2016) showed that in the northern Tien Shan between 1955/56 and 1975 glacier recession
66 rates were comparable with the 1990-2008 period and in the 1970s, they were 2-3 times higher.
67 The earlier data in this study, however, were derived from the Catalogue of Glaciers of the
68 USSR based on the aerial photography and topographic maps which were not preserved and,
69 therefore, assessment of uncertainty in the earlier data was problematic.

70 The review of the existing studies (Table 1A) shows that although there were many assessments
71 of glacier change in the Tien Shan, given its strong spatial variability, it is important to generate
72 up-to-date detailed regional assessments of glacier change over different time periods for the
73 regions which were not examined so far using materials which enable uncertainty assessment.

74 One of the glacierized regions of the Tien Shan where glacier change has not been documented
75 in detail is the basin of the River Tekes in the Central Tien Shan within the national borders of
76 Kazakhstan (Fig. 1). The Tekes is a transboundary river originating in Kazakhstan, crossing into
77 China where, in confluence with the River Kash, it forms the River Ile, which, in turn, returns to
78 Kazakhstan as a major source of water for irrigation and the nourishment of Lake Balkhash. The



79 Tekes is nourished by snow and glacier runoff and, given the current requirements for water in
80 both countries, it is important to assess changes in the extent of glaciers in its basin.
81 The history of glacier research in the Tekes basin dates back over a century when Merzbacher in
82 1904 and 1905 described two large glaciers in the upper reaches of the Bayankol River on the
83 northern slopes of the Katta-Ashutor and the Saryjaz which were catalogued as Mramornaya
84 Stena (No 94), Simonov (No 89) and Bayankol (No 91) glaciers in the Catalogue of Glaciers of
85 the USSR (Vilesov, 1969). The first larger scale assessment was conducted in 1915,
86 documenting 74 glaciers in the Kazakhstani sector of the Tekes basin with the combined area of
87 116 km² and this was followed by a comprehensive inventory of 1956 which provided data for
88 the Catalogue of Glaciers of the USSR (Vilesov; 1969). More recently, Vilesov (2006) reported
89 15.8 % (0.45% a⁻¹) glacier area reduction between 1956 and 1990. Xu et al. (2015) reported a
90 reduction of 18% (0.37 % a⁻¹) in the Chinese sector of the Tekes basin between 1960 and 2009,
91 which is higher than in the neighbouring Saryjaz region (Osmonov et al., 2013). There are no
92 post-1990 assessments of glacier change in the Kazakhstani sector of the Tekes basin.
93 Glacier outlines from the 1999-2003 period are available from the Randolph Glacier Inventory
94 5.0 (RGI5.0; http://www.glims.org/RGI/rgi50_dl.html). These outlines were generated by the
95 Glacier Area Mapping for Discharge from the Asian Mountains (GAMDAM) project using
96 manual mapping of glaciers on the Landsat imagery (Nuimura et al., 2015). Although the Tekes
97 basin was included in the GAMDAM inventory, the main purpose of GAMDAM was to derive
98 the extent of glacierized area for the High Asia and its much larger geographical units rather and,
99 therefore, no analysis for the Tekes basin is presented.
100 The objectives of this paper are: (i) to present inventories of glaciers derived from the Landsat
101 imagery for the Kazakhstani sector of the Tekes basin for 1992 and 2013; (ii) using a sub-
102 sample of glaciers, analyse changes in their extent between 1976, 1992 and 2013 and compare
103 the retreat rates; (iii) analyse changes in the extent of glacierized area and discuss them in the
104 context of climatic change and variability.



105

106 **2 Study area**

107 In the Kazakhstani sector of the Tekes basin, glaciers are located between 42°43'N and 40°16'N
108 and 79°13'E and 80°20'E on the northern macroslopes of the Terskey Alatau and Saryjaz Ridges,
109 on the western macroslope of the Meridional Ridge and in the Katta Ashutor Ridge (Fig. 1).
110 Elevations in the Terskey Alatau are mostly within 4200-4400 m a.s.l. range increasing to 5000-
111 5200 m in the Katta Ashutor and 5700-6100 m in the Saryjaz. In the Meridional Ridge,
112 elevations increase from 4000 m at the source of the Narynkol River to about 6000 m in the
113 south (Fig. 1).

114 According to the Catalogue of Glaciers of the USSR (Vilesov, 1969), in 1956 there were 152
115 glaciers with a combined area of 143.0 km² in the study area. The largest glaciers were located in
116 the Katta-Ashutor and the Saryjaz (e.g. Simonov, Bayankol, Mramornaya Stena with individual
117 areas of 28.1 km², 6.9 km², and 22.5 km² respectively) and on the northern macroslope of the
118 Meridional Ridge (e.g. Sauruksaiskiy (No 104), 7.9 km²). In all, in 1956, there were three
119 compound valley glaciers with a combined area of 58.5 km² and position of glacier tongues at
120 approximately 3350 m, 21 valley glaciers with a combined area of 54.4 km² and 19 cirque-valley
121 glaciers with a combined area of 14.0 km². The valley glaciers descended to approximately 3550
122 m. There were 27 cirque and 38 hanging glaciers with the combined areas of 6.9 km² and 5.6
123 km² and two ice aprons (1.8 km²) and one flat-summit (0.2 km²) glaciers.

124 The climate of the area is characterised by strong seasonal variations in atmospheric circulation
125 dominated by the western extension of the Siberian anticyclone in winter whose influence is
126 stronger in the valleys and diminishes with altitude giving way to the westerly flow
127 (Panagiotopoulos et al., 2005). The thermal Asiatic depression dominates in summer and the
128 westerly flow in spring and autumn with frequent depressions in September-October. These
129 changes predetermine strong seasonal fluctuations in temperature and precipitation (Fig. 2).



130 In winter, the combined effect of the Siberian anticyclone and high elevations results in low
131 temperatures whose December-January-February (DJF) means range between -10.8°C at 1800 m
132 at Narynkol meteorological station (Fig. 2; Table 1) and about -20°C at 3600-4000 m. The June-
133 July-August (JJA) mean temperature is 15.2°C at Narynkol decreasing to $2-4^{\circ}\text{C}$ at the glacier
134 tongue elevation where positive air temperatures are observed between early June and early
135 September. The ablation season is normally limited to JJA. Annual precipitation increases from
136 about 390 mm at Narynkol to 1000-1200 mm at the glacier elevation of 3600-4000 m (Vilesov,
137 1969). Precipitation maximum is observed in late spring - summer while winter precipitation is
138 low (Fig. 2; Table 1). At Narynkol, the May-August precipitation was 217 mm accounting for
139 56% of the annual total while DJF precipitation is 35 mm accounting for 9%. Accumulation
140 occurs throughout the year.

141

142 **3 Data and methods**

143 **3.1 Satellite imagery and glacier mapping**

144 Changes in glacierized area were assessed for the Kazakhstani sector of the Tekes River basin
145 (Fig. 1) using Landsat imagery from 1992 and 2013 (Table 2). Earlier KH-9 Hexagon imagery
146 was available for January 1976 and used for a limited number of glaciers whose tongues were
147 free of snow cover due to the strong negative precipitation anomalies in 1975 which was the
148 driest year on record with annual precipitation two standard deviations below the record mean
149 (see Fig. 9). Scenes from the same acquisition were used by Pieczonka and Bolch (2015) for the
150 calculation of geodetic mass balance using satellite imagery in the Tien Shan.

151 For 1992 and 2013, areas of 118 glaciers were mapped of which the largest was 21.3 km^2 and the
152 smallest was 0.01 km^2 . Four Landsat scenes (Table 2) were obtained from the US Geological
153 Survey (USGS; <http://glovis.usgs.gov/>) in the Universal Transverse Mercator (UTM) zones 44
154 WGS 84 projection. All Landsat images were acquired under [nearly] cloud-free conditions. The
155 2013 image was acquired at the end of the ablation season. The 1992 image was obtained at the



156 middle of the ablation season, however, at the time of image acquisition glacier tongues were
157 free of seasonal snow and the image was suitable for glacier mapping.

158 Glacier outlines were mapped using Landsat bands 7, 5, 3 for 1992 and 2013 and 8
159 (panchromatic) for 2013. Manual on-screen mapping was used despite the advantages of
160 automated mapping demonstrated by Paul et al. (2009; 2013). This is because relative error
161 strongly increases with decreasing glacier area (Paul et al., 2013; Fischer et al., 2014) and with
162 the presence of debris cover (Bhambri et al., 2011; Bolch et al., 2008; Racoviteanu et al., 2008;
163 Frey et al. 2012; Paul et al., 2013). Paul et al. (2013) and Fischer et al. (2014) have shown that
164 the bias significantly increases for glaciers with areas less than 1 km², which constitute 21% of
165 all glaciers in the Tekes basin, reducing the advantages of automated techniques. For the same
166 reasons, manual mapping of glacier boundaries was used in the GAMDAM inventory (Nuimura
167 et al., 2015) and by Narama et al. (2010) for the inventory focusing on the western, central and
168 northern Tien Shan. To assist manual delineation of debris-covered snouts, the higher-resolution
169 imagery from Google Earth was inspected in conjunction with the Landsat images.

170 Most glaciers in the study area have clearly defined ice divides but, where required, ASTER
171 DEM obtained from ASTER Global Digital Elevation Model site
172 (<http://gdem.ersdac.jspacsystems.or.jp/>) was used to delineate the upper boundaries. This
173 delineation was consistent with that used in the Catalogue of Glaciers of the USSR (Vilesov,
174 1969) enabling a comparison of glacier change since 1956. It was assumed that the upper
175 boundaries of the glaciers did not change between 1992 and 2013. The areas of emerging rocks
176 in the upper sections of glaciers were mapped and their areas were deduced from the glacier area.
177 For glaciers that fragmented between 1992 and 2013, combined areas were recorded. There were
178 no known surging glaciers in the study region.

179 Tongues of 28 glaciers were clearly visible on KH9-Hexagon image (Table 2) allowing mapping
180 of their positions. Technical details of KH-9 Hexagon imagery, declassified in 2002, are
181 provided by Surazakov and Aizen (2010) and Burnett (2012). The sensor used a frame mapping



182 camera with a 23 x 46 cm frame and a focal length of 30.5 cm. The KH9 scenes covered areas of
183 125 x 250 km² on a scale of 1:600,000 at an altitude of ~170 km (Burnett, 2012). The images
184 were provided by the USGS with a scan resolution of about 14 μm. The pre-processing of the
185 KH-9 image, involving the removal of internal film distortions based on reseau crosses, has been
186 done following Pieczonka et al. (2013). The KH-9 image were co-registered to the orthorectified
187 Landsat TM and Landsat OLI TIRS images using a network of GCPs that have been collected
188 from the Landsat images. This procedure was carried out using ERDAS Imagine 9.0 software
189 and produced the maximum root-mean-square error (RMSE_{xy}) values of 5.1 m and 4.8 m
190 respectively. Following the co-registration, ice margins in the glacier ablation zones were
191 manually derived from the KH-9 images. Glacier margins in the accumulation zone were
192 delineated from the Landsat imagery. Figure 3 shows an example of a comparison of glacier
193 outlines from the Landsat and KH-9 images.

194

195 **3.2 Quantification of uncertainty**

196 **3.2.1 Landsat images**

197 For each scene, the accuracy of the orthorectification was verified using a network of interactive
198 ground control points (GCPs) obtained from 1:50000 maps using clearly identifiable terrain
199 features whose location did not change. For each glacier, two uncertainty terms have been
200 calculated resulting from the uncertainty of orthorectification and from identification of the
201 glacier margins. The uncertainty of orthorectification was calculated following Granshaw and
202 Fountain (2006). A buffer, with a width of half of the RMSE_{x,y} was created along the glacier
203 outlines and the uncertainty term was calculated as an average ratio of the original glacier areas
204 to the areas with a buffer increment. The values of RMSE_{x,y} were 25 m and 29 m for the Landsat
205 TM scenes and 14.5 m and 14 m for Landsat OLI TIRS scenes resulting in a mean uncertainty of
206 ±18.1% and ±12.3% for 1992 and 2013 respectively. The uncertainty of glacier margin
207 identification was taken as 3.5% for each image following a multiple digitization study by Paul



208 et al. (2013). The total mean uncertainties of glacier map area calculation were $\pm 18.6\%$ and
209 $\pm 13\%$ in 1992 and 2013 respectively.

210 To estimate uncertainty of glacier area change, the 1992 and 2013 scenes were co-registered
211 using 15-20 well-identifiable points on the images. The maximum value of $RMSE_{x,y}$ was 5 m.
212 The uncertainty of co-registration was calculated using the buffer method resulting in an average
213 uncertainty of $\pm 3.1\%$ and $\pm 4.1\%$ for 1992 and 2013 respectively. The combined uncertainty of
214 co-registration and $\pm 3.5\%$ uncertainty of glacier margin identification was $\pm 7.5\%$.

215 Debris cover on glacier snouts is a major source of uncertainty in glacier mapping (Bolch et al.,
216 2008; Racoviteanu et al., 2008; Frey et al. 2012; Paul et al., 2013). We considered and rejected
217 the frequently used practice of inflating the uncertainty term of glacier margin identification for
218 the debris-covered sectors of glacier tongues (e.g. Frey et al., 2012; Shahgedanova et al., 2014).
219 This is because debris cover is extensive on the tongues of the largest glaciers (e.g. Bayankol,
220 Mramornaya Stena, Simonov; Fig. 7 further in the text) where it does not merge periglacial
221 landforms and a close inspection and the use of higher resolution Google Earth imagery enables
222 the delineation of glacier margins. On other glaciers, the extent of debris cover is significantly
223 smaller than in the neighbouring Saryjaz region (Osmonov et al., 2013) enabling its manual
224 delineation.

225

226 **3.2.2 KH-9 images**

227 To estimate the uncertainties of mapping of glacier area from the 1976 KH-9 imagery, we
228 considered the uncertainty of orthorectification and the uncertainty of margin delineation by
229 individual operator ($\pm 3.5\%$). The former was calculated using the buffer method with the width
230 equal to the half of the KH-9 pixel of 7.6 m. The combined uncertainty was $\pm 4.3\%$.

231 The uncertainty of changes in glacier area were calculated using the uncertainty of co-
232 registration of KH-9 and Landsat images and the uncertainty of glacier margin delineation. The



233 combined uncertainties were $\pm 5.6\%$ for the 1976 and 1992 images and $\pm 5.8\%$ for the 1976 and
234 2013 images.

235

236 **3.3 Meteorological data**

237 Monthly statistics for air temperature and precipitation from the Narynkol station ($42^{\circ}43'N$; 80
238 $^{\circ}11'E$; 1806 m a.s.l.) was used (Fig. 1; Table 1). The station is located in a wide valley (about 20
239 km in cross-section) of the River Tekes, which has west-east orientation. The station was
240 established in 1947 and moved twice: In 1953, it was moved by 50 m east and in 1975, it was
241 moved 500 m north-east of its original location (Aliyakbarova, 2004). Currently, the station is
242 located at the south-eastern edge of a village Narynkol in which one-storey buildings
243 predominate. The nearest buildings are positioned 50-70 m away from the station and their
244 heights do not exceed 8-13 m. Although there has been no assessment of urban heat island in
245 Narynkol, the heights of the buildings suggest that it should be low. The Tretyakov rain gauge
246 was introduced in 1951 replacing a Naphier rain gauge (Aliyakbarova, 2004). In this study, we
247 used temperature for the 1947-2015 period and precipitation for the 1952-2015 period.

248 Several statistical tests have been used to examine temporal variability in the temperature and
249 precipitation records. In addition to the widely applied linear trend analysis, the Cumulative Sum
250 Control Chart (CUSUM) test (Mansell, 2003) and Mann-Kendall sequential test (Sneyers, 1990)
251 were applied. Both tests are used to identify approximate time of beginning of a trend or change
252 points in time series.

253

254 **4 Results**

255 **4.1 Glacier change between 1992 and 2013**

256 In 1992, there were 118 glaciers in the study region with a combined map area of $121.4 \pm 9.2 \text{ km}^2$
257 and by 2013, their area declined to $105.0 \pm 5.5 \text{ km}^2$. The total area loss was $16.4 \pm 5.9 \text{ km}^2$ or



258 13.5±7.5%. The rate of area reduction was 0.78 km² a⁻¹ or 0.64% a⁻¹. Six glaciers separated and 8
259 glaciers disappeared.

260 Similar to other regions (e.g. Kutuzov and Shahgedanova, 2009; Narama et al., 2010; Xu et al.,
261 2015), larger glaciers lost smaller proportions of their areas (Fig. 4 and Table 3). The absolute
262 area loss by glaciers of 1-2 km² and 2-5 km² classes were higher than that of the glaciers in 0.01-
263 1 km² class. However, due to a large number of glaciers in the 0.01-1 km² class, their combined
264 area loss was the highest (Table 3). In 1992, the smallest glaciers occupied 21.2% of the total
265 glacierized area and in 2013, they accounted for 52.8% of area loss. All glaciers, which melted
266 completely, ranged in size between 0.02 km² and 0.19 km². The largest glaciers (>5 km²)
267 accounted for 55.9% the total glacierized area in 1992 and in 2013, they accounted for 20.9% of
268 total area loss. However, the absolute area loss by the six largest glaciers was relatively small
269 and close to the uncertainty of measurement.

270 The largest glaciers belonged to the compound-valley type (Table 4; Fig. 5). Three of these
271 glaciers (Mramornaya Stena, Simonov and No 104) are located on the northern slope of the
272 Saryjaz and in the Meridional Ridge respectively. The accumulation zones of these glaciers are
273 positioned at higher elevations reaching 4400 – 6150 m a.s.l. Tongues of three largest glacier –
274 Marmornaya Stena, Bayankol and Simonov – have an extensive debris cover which slows down
275 their retreat (Fig. 7 further in the text). Their low recession rates are consistent with the slow
276 wastage reported by Osmanov et al. (2013) for glaciers of similar size in the southern sector of
277 the Saryjaz. The largest absolute loss characterised valley glaciers (Table 4; Fig. 5). Cirque
278 glaciers exhibited higher relative loss despite their shaded positions. This was probably due to
279 their smaller areas which averaged 0.21 km² and location at lower elevations between 3440 m
280 and 4500 m in contrast to the valley glaciers which averaged 2.1 km² extending from 3550 m to
281 5840 m. The largest relative loss was characteristic of ice aprons followed by the flat-summit
282 glaciers. Although there are only three glaciers of these types in the study area, the high rates of
283 their recession are consistent with the trend reported by Kutuzov and Shahgedanova (2009) for



284 the Terskey-Alatoo and can be attributed not only to their small size but also to the fact that
285 glaciers of these types have large marginal areas and recession occurs along the whole margin
286 rather than relatively narrow glacier terminus.

287 Most glaciers in the region have northern aspect. Out of 118 glaciers, 55 faced north, 18 north-
288 west and 20 north-east and this is why the combined area loss was highest for the glaciers with
289 northern aspect accounting for $8.5 \pm 2.3 \text{ km}^2$. Glaciers with southern and eastern aspect, of which
290 there are only fourteen, lost the highest proportions of their area (Fig. 6).

291

292 **4.2 Glacier change between 1976, 1992 and 2013**

293 The combined area of 28 glaciers measured from the KH-9 Hexagon image from 1976 was
294 $80.1 \pm 3.0 \text{ km}^2$ (Table 5 a). Glaciers in this sample were larger than on average across the region
295 with a mean area of 2.86 km^2 . By 1992, their combined area had decreased to $73.5 \pm 4.7 \text{ km}^2$
296 (60.5% of the total glacier area in the basin) and by 2013, to $67.3 \pm 3.1 \text{ km}^2$ (64% of the total
297 glacier area in the basin). The rates of glacier wastage are shown in Table 5 b. Figure 7 illustrates
298 the recession of three large glaciers in this region while Figure 3 illustrates changes in areas of
299 smaller glaciers. The recession rates were slightly higher in 1976 - 1992 period than in 1992-
300 2013 although the differences are close to the measurement uncertainty.

301

302 **4.3 Changes in temperature and precipitation**

303 According to the climatic data from the Narynkol station, positive trends in temperature
304 significant at 0.05 level were observed in all seasons (Fig. 8; Table 1). The strongest increase
305 occurred in autumn and winter. The strongest trend of $0.58^\circ\text{C}/10 \text{ a}^{-1}$ was observed in November
306 while in October and December and February temperature increased at a rate of approximately
307 $0.30\text{-}0.45^\circ\text{C}/10 \text{ a}^{-1}$. In January, when the Siberian anticyclone is at its strongest, the trend was
308 weaker at $0.20^\circ\text{C}/10 \text{ a}^{-1}$. In September, temperature increase occurred at a rate of $0.23^\circ\text{C}/10 \text{ a}^{-1}$.
309 The summer temperature time series was characterised by weaker interannual variability than



310 other seasons as indicated by the lowest value of the coefficient of variation (CV). The
311 application of the CUSUM and Mann-Kendall sequential tests confirmed the presence of a
312 continuous positive trend without significant abrupt changes in all time series.
313 None of the precipitation time series including annual, those for the standard meteorological
314 seasons or for glacier mass balance seasons (defined as September-May and JJA) exhibited
315 linear trend significant at 0.05 level. Both CUSUM and Mann-Kendell sequential tests indicate
316 presence of the opposite trends in the annual precipitation time series before and after 1976-1977
317 resulting from changes in the summer and spring precipitation (Fig. 9; Table 1). Strong negative
318 anomalies in annual precipitation were observed in 1975-1977. The 1975 annual total was two
319 standard deviations below the record mean, while in 1977 the annual precipitation values were
320 close to this threshold. Following the reversal of the negative trend, annual precipitation totals
321 were increasing until 1993, however, a number of dry years occurred in the 2010s and in
322 particular, 2012 was the second driest year on record with the annual total of 277 mm (Fig. 9).
323 Similarly to the dry period of the late 1970s, the decline in annual totals in the 2010s was due to
324 the reduction in spring precipitation. Both the dry periods of the late 1970s and 2012-2014
325 coincided with the period of positive anomalies in summer temperature. There is no statistically
326 significant difference between 1952-1977 and 1977-2015 annual and seasonal precipitation totals
327 (Table 1). There is also no statistically significant difference between precipitation averaged over
328 1976-1992 and 1992-2013 periods, 363 ± 57 mm and 404 ± 77 mm respectively, over which the
329 retreat rates of 28 glaciers were measured.

330

331 **5 Discussion**

332 **5.1. Glacier change between 1992 and 2013**

333 Glaciers in the Kazakhstani sector of the Tekes River basin have lost $13.5 \pm 7.5\%$ of their area
334 over the 1992 - 2013 period retreating at a rate of $0.60 \pm 0.3 \%$ a^{-1} . In comparison with the
335 changes observed in other glacierized regions of the northern Tien Shan in approximately the



336 same time period, glacier recession in the Tekes basin proceeded at a slower rate. In the recent
337 assessment by Severskiy et al (2016), the retreat rate in the Zailiyskiy Alatau in the 1990-2008
338 period was reported as 0.89 \% a^{-1} while in the Djungarskiy Alatau the retreat rate was even
339 higher at 1.1 \% a^{-1} between 1990 and 2011. This difference can be attributed to the different size
340 of glaciers. In the Tekes basin, areas of three large glaciers with extensive debris cover
341 (Mramornaya Stena, Simonov and Bayankol; Fig. 7), accounting for 40% and 45% of the
342 combined glaciated area in 1992 and 2013 respectively, did not change beyond the error of
343 measurement ($2.5 \pm 5.0\%$). This is similar to the Saryjaz Range, located south of the Tekes basin,
344 where glaciers, which are larger and positioned at higher elevation, retreated at $0.19\% \text{ a}^{-1}$ leading
345 to the overall reduction by $3.7 \pm 2.7\%$ in the 1990-2010 period (Osmonov et al., 2013; Table 1A).
346 The combined area of all other glaciers, excluding the three largest, in the Tekes basin declined
347 by $20.8 \pm 7.5 \text{ \%}$ or $0.99 \pm 0.36 \text{ \% a}^{-1}$. These statistics are comparable with the results by Severskiy
348 et al. (2016) for other regions of the northern Tien Shan most of which feature smaller glaciers.
349 The mean retreat rates for all glaciers in the sample is very close to 0.57 \% a^{-1} reported by
350 Narama et al. (2010) for the central and northern Tien Shan for a shorter period of 2000-2008
351 (Table 1A).
352 The importance of the impact of debris cover on the retreat rates of glaciers can be illustrated by
353 a comparison of two individual glaciers of a similar size, type and aspect: Bayankol (6.2 km^2)
354 which has extensive debris and Sauruksaisky (6.8 km^2) which has a clear snout. While the area
355 of Bayankol declined by $2.0 \pm 5.0\%$, the area Sauruksaisky declined by $11.0 \pm 5.2\%$. Extensive
356 debris cover on the glaciers of the Saryjaz was identified by Osmonov et al. (2013) as one of the
357 factors predetermining their slow retreat. Pieczonka and Bolch (2105) also highlighted lower
358 retreat rates of debris-covered glaciers in the Kokashal-Too, Tomur and Inylchek regions in
359 comparison with other glaciers in these regions.
360 As in many other regional studies (Kutuzov and Shahgedanova, 2009; Narama et al., 2010),
361 smaller glaciers retreated faster and lost higher proportions of their area. Changes in the extent of



362 the largest glaciers with areas in excess of 5 km² between 1992 and 2013 were close the
363 uncertainty of measurements (Table 3) and changes in the extent of three largest compound-
364 valley glaciers were insignificant (Table 4). In contrast to other studies (e.g. Kutuzov and
365 Shahgedanova, 2009), cirque glaciers lost smaller proportions of their area than valley glaciers
366 but this is probably due to position of the accumulation zones of valley glaciers at higher
367 elevations.

368

369 **5.2. Glacier change between 1956 / 1976 and 2013**

370 A sub-sample of 28 glaciers was used to assess temporal changes in glacier recession rates. This
371 sub-sample included larger than average glaciers whose relative area loss was lower at 8.4 ±
372 5.9% than the regional value in the 1992-2013. Between 1976 and 2013, these glaciers retreated
373 at a rate of 0.43±0.16 % a⁻¹ and lost 16.0±5.8% of their combined area. Analysis of retreat rates
374 between 1976 – 1992 (0.52±0.35% a⁻¹) and 1992 – 2013 (0.40±0.28% a⁻¹) indicated that there
375 was no acceleration in the glacier recession rates and that the temporal changes in the recession
376 rates are within the uncertainty of the measurements (Table 5b). This result is consistent with the
377 low temporal variability in the glacier recession rates reported by Severskiy et al. (2016) for the
378 Djungarskiy and Zailiyskiy Alatau and contrasts the conclusions by Narama et al. (2010) who
379 reported a slight acceleration in glacier retreat rates in central and northern Tien Shan.

380 According to the Catalogue of Glaciers of the USSR (Vilesov, 1969), the combined area of the
381 same 28 glaciers was 86.3 km² in 1956 and, therefore between 1956 and 1976, these glaciers
382 were retreating at a rate of 0.36 % a⁻¹ (Table 5b). Uncertainty analysis is not possible with regard
383 to the 1956 data, however, the 1956-1976 retreat rate is close to those observed in the following
384 decades and the difference appears to be close the uncertainty of measurement of glacierretreat
385 using satellite imagery. Between 1956 and 2013, the glaciers lost 22.0% of their combined area
386 retreating at a rate of 0.39 % a⁻¹. This is very close the 0.37±0.22 % a⁻¹ retreat rate reported by
387 for the Chinese sector of the Tekes basin for the 1960 – 2009 period by Xu et al. (2015).



388

389 **5.3. Comparison of the 1976 data with the data published in the Catalogue of Glaciers of**
390 **the USSR**

391 The Catalogue of Glaciers of the USSR (Vilesov et al., 1969) presented results from a large scale
392 inventory conducted in the Tien Shan in the 1950s-1960s which are often used as the benchmark
393 data in the evaluation of glacier wastage (e.g. Vilesov et al., 2006; Bolch et al., 2007, Severskiy
394 et al., 2016). A direct assessment of the accuracy of the Catalogue data by Shahgedanova et al.
395 (2010) for the Altai Mountains by re-mapping a sample of glaciers on the aerial photographs
396 used in the compilation of the Catalogue of Glaciers (Dushkin, 1974) indicated that the
397 combined glacier area published in the Catalogue was 5.5% higher than the re-mapped area and
398 although for individual glaciers did not exceed 12%. By contrast, an assessment for the Kodar
399 Mountains, eastern Siberia by Stokes et al. (2013) revealed that over 50% difference existed
400 between areas of individual glaciers presented in the Catalogue of Glaciers (Novikova and
401 Grinsberg, 1972) and the re-mapped data and a number of glaciers were missing from the
402 Catalogue. While similar re-assessment is impossible for the northern Tien Shan including the
403 Tekes basin because the aerial photographs were not preserved, the consistent rate of change
404 between 1956-1976 and the later time periods, which is in line with temperature change (section
405 5.4), indicates that the Catalogue data are unlikely to contain major error with regard to the
406 combined area of glaciers. However, within the area covered by the KH9 Hexagon imagery, one
407 glacier with area of 0.6 km² as in 1976 was missing from the Catalogue of Glaciers (Vilesov,
408 1969).

409

410 **5.4. Comparison with the RGI5.0 / GAMDAM**

411 A comparison of our results with those published by RGI5.0 using data from the GAMDAM
412 inventory (Nuimura et al., 2015) indicated that glacier area in the Tekes basin was
413 underestimated by RGI5.0 / GAMDAM in comparison with this study. The methodology



414 adopted by Nuimura et al. (2015) explicitly excludes glaciers located on the slopes with gradient
415 exceeding 40° which are considered to be steep headwalls without permanent ice cover. While
416 this approach may be justified in other regions of the High Asia, in the Tekes basin, it results in
417 the exclusion of the accumulation zone of glaciers which were considered a part of glacierized
418 area both in this study and in the Catalogue of Glaciers (Vilesov et al., 1969). It also makes
419 comparisons with other regions problematic as none of the regional glacier inventories in the
420 Tien Shan (Table 1A) use this methodology.

421 Figure 10 illustrates the discrepancy between our analysis and RGI5.0 / GAMDAM data. The
422 combined map area of glaciers 89 (Simonov), 90, 91 (Bayankol) and 94 (Mramornaya Stena)
423 was 34.7 km² in 1999 – 2003 according to the RGI5.0 / GAMDAM while smaller glaciers No 92
424 and 93 are not accounted for. According to our measurements, the combined area of these six
425 glaciers was 47.4 ± 1.9 km² in 2013 after the removal of rock outcrops. The difference of 12.7
426 km² constitutes 12.1% of the combined glacier area in the Tekes basin in 2013. Examination of
427 the Landsat and high-resolution SPOT imagery (Figure 10) shows that crevasses indicating the
428 presence of ice were notable in the accumulation zones of glaciers (e.g. Glacier N 94) excluded
429 by RGI5.0 / GAMDAM. While there were no radar surveys of ice thickness in the accumulation
430 zones of glaciers in the Tekes basin, the radar surveys on the Sary-Tor glacier in the Ak-Shirak
431 massif (Petrakov et al., 2014) showed that ice thickness on the very steep slopes was 20-40 m.
432 Similar values were obtained by Kuzmichonok et al. (1992) for the Abramov glacier.

433 In addition, 59 small glaciers (including those separated from the larger glaciers) with a
434 combined area of 11.8 km² are not accounted for in RGI5.0 / GAMDAM. Overall, the combined
435 glacier area presented in RGI5.0 / GAMDAM for 1999 – 2003 is lower by approximately 25 km²
436 or 24% than the combined area a decade later in 2013.

437

438 **5.5. Changes in temperature and precipitation.**



439 As in many other regions of the Tien Shan (Farinotti et al., 2015), increasing summer
440 temperatures appear to be the main driver of glacier retreat. The JJA temperatures have been
441 increasing steadily at a rate of 0.18°C per 10 years in the study area since 1953 (Fig. 8) with
442 linear trends explaining 25% of the total variance (Table 1). Correlation analysis has not revealed
443 any significant impacts of either global (e.g. El Nino – Southern Oscillation) or Northern
444 Hemisphere (Panagiotopoulos et al., 2002) teleconnections on temperature. The rate of change is
445 consistent with changes in summer temperature observed in other regions of the Tien-Shan
446 (Aizen et al., 1997; Kutuzov and Shahgedanova, 2009; Osmonov et al., 2013; Pieczonka and
447 Bolch, 2015). The strongest warming was observed in the Tekes basin in autumn and winter and
448 similar results were reported by Duethmann et al. (2015) for the Aksu River basin. Of all autumn
449 months, the highest rate of warming occurred in November (0.58°C per 10 years) and the lowest
450 in September (0.23°C per 10 a⁻¹). Annual temperature was increasing at a rate of 0.30°C per 10
451 years and this is consistent with 0.34°C per 10 years warming reported by Wang et al. (2011) for
452 the Chinese sector of the Ile River basin.

453 The observed warming is likely to lead to an increase in the proportion of liquid precipitation
454 both, at higher elevations in summer when glaciers receive most of their nourishment, and in the
455 transitional months (May and September) in the future. These changes may reduce accumulation
456 and increase ablation through higher temperatures in the current ablation season and its extension
457 into the transitional months.

458 There were no statistically significant linear trends in precipitation in any season although the
459 records exhibited strong interannual variability. Similar results were reported for other regions
460 of the Tien Shan by Aizen et al. (1997), Bolch (2007), Kutuzov and Shahgedanova (2009) and
461 Sorg et al. (2012) while Krysanova et al. (2015) reported positive trends in April-September
462 precipitation in the Aksu River basin in Kyrgyzstan and China. Precipitation was declining in the
463 1952–1977 period, increasing between 1977 and 1993 and then again decreasing until 2015 with
464 a very dry year of 2012 (Fig. 9). However, to date this variability did not seem to affect glacier



465 recession rates significantly on the time scale of two decades as the retreat rates for 1976-1992
466 and 1992-2013 were close with the differences within the error of measurement (Table 5) most
467 likely because there was no statistically significant difference between the average precipitation
468 values for these periods. The use of finer time steps in the analysis of glacier change may be able
469 to detect an impact of precipitation variability. Thus Severskiy et al. (2016) showed that the
470 highest glacier recession rates were observed in the northern Tien Shan between 1975 and 1979,
471 a period that was the driest on record (Fig. 9), exceeding those in 1990-2008 by the factor of two.
472 More recently, strong negative anomalies in annual precipitation driven by reduction in the
473 spring snowfall were observed in 2012-2014. The combination of a continuous increase in
474 summer temperatures and negative anomalies in spring and summer precipitation are likely to
475 have accelerated glacier wastage in the Tekes basin in the 2010s similarly to its acceleration in
476 the mid-1970s.

477

478 **6 Conclusions**

479 In the Kazakhstani sector of the Tekes basin, glaciers lost $13.5 \pm 7.5\%$ in the 1992-2013 period.
480 This retreat rate appears to be slower than in many other regions of the Tien Shan in the same
481 period because of the presence of several large glaciers, whose areas remained unchanged, in the
482 sample. There was no significant change in the recession rates over time. A small reduction in
483 the recession rates in 1992-2013 in comparison with 1976-1992 appears to be within the
484 accuracy of our measurements: $0.40 \pm 0.28\% \text{ a}^{-1}$ versus $0.52 \pm 0.35\% \text{ a}^{-1}$. A steady increase in
485 temperature is a driving factor of glacier recession. The observed variability in precipitation
486 appears not to have a strong impact on glacier recession rates averaged over 15-20 year periods
487 although the influence of precipitation changes may be better detected if glacier change is
488 assessed at a finer time step. Positive temperature trends were observed in spring and autumn
489 month with the particularly high warming rates in autumn. This warming is likely to result in the



490 extension of the melting season and higher proportion of liquid precipitation leading to further
491 and potentially faster glacier recession in the future.

492

493 *Acknowledgements.* This work was conducted as a part of the project “Climate Change, Water
494 Resources and Food Security in Kazakhstan” funded by Newton - al-Farabi Fund (grant No
495 172722855).

496

497 **References**

498 Aizen, V.B., Aizen, E.M., Melack, J.M., and Dozier, J.: Climatic and hydrological changes in the
499 Tien Shan, Central Asia, *Journal of Climate*, 10 (6), 1393–1404, 1997

500 Aizen, V.B., Kuzmichenok, V.A., Surazakov, A.B., and Aizen, E. M.: Glacier changes in the
501 central and northern Tien Shan during the last 140 years based on surface and remote-sensing
502 data, *Annals of Glaciology*, 43, 202–213, 2006.

503 Aizen, V.B., Kuzmichenok, V.A., Surazakov, A.B., and Aizen, E.M.: Glacier changes in the
504 Tien Shan as determined from topographic and remotely sensed data, *Global and Planetary
505 Change*, 56, 328-340, doi:10.1016/j.gloplacha.2006.07.016, 2007.

506 Aliyakbarova, N.R. (ed.): *Spravochnik po klimatu Kazakhstana* (Reference book on climate of
507 Kazakhstan), Issue 14, Part 1, Almaty, 563 pp, in Russian, 2004.

508 Bhambri, R., Bolch, T., Chaujar, R.K., and Kulshreshtha, S.C.: Glacier changes in the Garhwal
509 Himalaya, India, from 1968 to 2006 based on remote sensing, *J. Glaciol.*, 57 (203), 543-556,
510 2011.

511 Bolch, T., Buchroithner, M., Pieczonka, T., and Kunert, A.: Planimetric and volumetric glacier
512 changes in the Khumbu Himalaya, Nepal, since 1962 using Corona, Landsat TM and ASTER
513 data, *J. Glaciol.*, 54 (187), 592-600, 2008.



514 Bolch, T.: Climate change and glacier retreat in northern Tien Shan (Kazakhstan/ Kyrgyzstan)
515 using remote sensing data, *Global and Planetary Change*, 56, 1–12,
516 doi:10.1016/j.gloplacha.2006.07.009, 2007.

517 Bolch, T.: Glacier area and mass changes since 1964 in the Ala Archa Valley, Kyrgyz Ala-Too,
518 northern Tien Shan, *Led i Sneg (Ice and Snow)*, 1 (129), 28-39, 2015.

519 Burnett, M.G.: Hexagon (KH-9) Mapping Program and Evolution. National Reconnaissance
520 Office, Chantilly, Virginia, 2012.

521 Desinov, L.V., and Konovalov, V.G.: Distancionny monitoring mnogoletnego regima oledenienia
522 Pamira (Monitoring of multiannual glacial regime in the Pamir using remote sensing), *Data of*
523 *Glaciological Studies*, 103, 129–134, in Russian, 2007.

524 Du, W., Li, J., Bao, A., and Wang, B.: Mapping changes in the glaciers of the eastern Tianshan
525 Mountains during 1977–2013 using multitemporal remote sensing, *Journal of Applied Remote*
526 *Sensing*, 8 (1), 1-15, doi:10.1117/1.JRS.8.084683, 2014.

527 Duethmann, D., Bolch, T.; Farinotti, D., Kriegel, D., Vorogushyn, S., Merz, B., Pieczonka, T.,
528 Jiang, T., Su, BD., and Guntner, A.: Attribution of streamflow trends in snow and glacier melt-
529 dominated catchments of the Tarim River, *Central Asia Water Resources Research*, 51(6), 4727-
530 4750, doi: 10.1002/2014WR016716, 2015

531 Dushkin, M.A. (ed.): *Katalog Lednikov SSSR, Altay i Zapadnaya Sibir', Gornyy Altay i*
532 *Verkhniy Irtysh, Basseyn reki Chuya*, Tom 15, Vypusk 1, Chast' 6 [Glaciers inventory of the
533 USSR. Altai and Western Siberia, Altai Mountains and the Upper Irtysh River, Chuya River
534 Basin]. Vol. 15. Issue 1, Part 6, Gidrometeoizdat, Leningrad, 60 pp., in Russian, 1974.

535 Farinotti, D., Longuevergne, L., Moholdt, G., Duethmann, D., Mölg, T., Bolch, T., Vorogushyn,
536 S., and Guntner, A.: Substantial glacier mass loss in the Tien Shan over the past 50 years, *Nature*
537 *Geoscience*, 8, 716–722, doi: 10.1038/ngeo2513, 2015.



- 538 Fischer, M., Huss, M., Barboux, C., and Hoelzle, M.: The new Swiss Glacier Inventory
539 SGI2010: Relevance of using high-resolution source data in areas dominated by very small
540 glaciers, *Arct. Antarct. Alp. Res.*, 46(4), 933-945, 2014.
- 541 Frey, H., Paul F., and Strozzi T.: Compilation of a glacier inventory for the western Himalayas
542 from satellite data: methods, challenges, and results, *Rem. Sens. Environ.*, 124, 832-843, 2012.
- 543 Granshaw, F.D., and Fountain A.G.: Glacier change (1958-1998) in the North Cascades National
544 Park Complex, Washington, USA, *J. Glaciol.*, 52 (177), 251-256, 2006.
- 545 Hagg, W., Mayer, C., Lambrecht, A., Kriegel, D., and Azizov E.: Glacier changes in the Big
546 Naryn basin, Central Tian Shan, *Global and Planetary Change*, 110, 40–50,
547 doi:10.1016/j.gloplacha.2012.07.010, 2013.
- 548 Holzer, N., Vijay, S., Yao, T., Xu, B., Buchroithner, M., and Bolch, T.: Four decades of glacier
549 variations at Muztagh Ata (eastern Pamir): a multi-sensor study including Hexagon KH-9 and
550 Pléiades data, *The Cryosphere*, 9, 2071–2088, doi:10.5194/tc-9-2071-2015, 2015.
- 551 Kaldybayev, A., Chen, Y., and Vilesov, E.: Glacier change in the Karatal river basin, Zhetysu
552 (Dzhungar) Alatau, Kazakhstan, *Annals of Glaciology*, 57 (71), 11- 19, doi:
553 10.3189/2016AoG71A005, 2016.
- 554 Khalsa, SJS.; Dyurgerov, M.; Khromova, T., Raup, B., and Barry, RG.: Space-based mapping of
555 glacier changes using ASTER and GIS tools, *IEEE Transactions on geoscience and remote
556 sensing*, 42 (10), 2177-2183, 2004.
- 557 Khromova, T.E., Dyurgerov, M.B., and Barry, R.G.: Late-twentieth century changes in glacier
558 extent in the Ak-shirak Range, Central Asia, determined from historical data and ASTER
559 imagery, *Geophysical Research Letters*, 30 (16), 1-5, doi:10.1029/2003GL017233, 2003
- 560 Khromova, T.E., Osipova, G.B., Tsvetkov, D.G., Dyurgerov, M.B., and Barry, R.G.: Changes in
561 glacier extent in the eastern Pamir, Central Asia, determined from historical data and ASTER
562 imagery, *Remote Sensing of Environment*, 102 (1–2), 24–32, doi:10.1016/j.rse.2006.01.019,
563 2006.



564 Kriegel, D., Mayer, C., Hagg, W., Vorogushyn, S., Duethmann, D., Gafurov, A., and Farinotti
565 D.: Changes in glacierisation, climate and runoff in the second half of the 20th century in the
566 Naryn basin, Central Asia, *Global and Planetary Change*, 110, 51–61,
567 doi:10.1016/j.gloplacha.2013.05.014, 2013.

568 Krysanova, V., Wortmann, M., Bolch, T., Merz, B., Duethmann, D., Walter, J., Huang, Sh.,
569 Tong, J., Buda, S., and Kundzewicz, Z.W.: Analysis of current trends in climate parameters,
570 river discharge and glaciers in the Aksu River basin (Central Asia), *Hydrological Sciences*
571 *Journal*, 60:4, 566-590, doi:10.1080/02626667.2014.925559, 2015.

572 Kutuzov, S., and Shahgedanova, M.: Glacier retreat and climatic variability in the eastern
573 Terskey-Alatoo, inner Tien Shan between the middle of the 19th century and beginning of the
574 21st century, *Global and Planetary Change*, 69, 59–70, doi:10.1016/j.gloplacha.2009.07.001,
575 2009.

576 Kuzmichenok, V.A.: Tekhnologiya i vozmozhnosti aerotopographicheskogo kartogrphirovaniya
577 izmeneniy lednikov (na primere oledeneniya khrebt Akshirak) (Methods and opportunities of
578 the aero topographic cartography in context of glaciers changes (e.g. Akshirak range glaciers),
579 *Data of Glaciological Studies*, 67, 80–87, in Russian, 1989.

580 Kuzmichenok, V.A., Vasilenko, E.V., Macheret, Yu.Ya., and Moskalevskiy, M.Yu.: Tolshchina
581 l'da i podlednyy rel'yef lednika Abramova po dannym nizkochastotnogo radiozondirovaniya
582 (The ice thickness and subglacial relief of Abramov glacier according to the data of low-
583 frequency radiosounding) *Materialy glyatsiologicheskikh issledovaniy (Data Glaciol. Stud.)*, 75,
584 63–68, in Russian, 1992.

585 Li, B., Zhu, A.X., Zhang, Y., Pei, T., Qin, C., Zhou, C.: Glacier change over the past 4 decades
586 in the middle Chinese Tien Shan, *Journal of Glaciology* 52 (178), 425–432,
587 doi:10.3189/172756506781828557, 2006.



- 588 Li, KM., Li, ZQ. Gao WY., Wang, L.: Recent glacial retreat and its effect on water resources in
589 eastern Xinjiang, Chinese Science Bulletin, 56 (33), 3596-3604, doi:10.1007/s11434-011-4720-
590 8, 2011.
- 591 Mansell, M.G.: Rural and Urban Hydrology. Thomas Telford, London, 411 pp, 2003.
- 592 Narama, C., Kaab, A., Duishonakunov, M., and Abdrakhmatov, K.: Spatial variability of resent
593 glacier area changes in the Tien Shan Mountains, Central Asia, using Corona (~1970), Landsat
594 (~2000), and (~2007) satellite data, Global and Planetary Change, 71 (1-2), 42–54,
595 doi:10.1016/j.gloplacha.2009.08.002, 2010.
- 596 Narama, C., Shimamura, Y., Nakayama, D., and Abdrakhmatov, K.: Recent changes of glacier
597 coverage in the western Terskey–Alatoo range, Kyrgyz Republic, using Corona and Landsat,
598 Annals of Glaciology, 43, 223–229, 2006.
- 599 Niederer, P., Bilenko, V., Ershova, N., Hurni, H., Yerokhin, S., Maselli, D.: Tracing glacier
600 wastage in the Northern Tien Shan (Kyrgyzstan/Central Asia) over the last 40 years, Climatic
601 Change, 86 (1–2), 227–234, doi:10.1007/s10584-007-9288-6, 2007.
- 602 Novikova, Z.S., and Grinberg, A.M.: Katalog lednikov SSSR, Lensko-Indigirskiy rayon,
603 Srednyaya Lena, Basseyny rek Chara i Vitim (Khrebet Kodar), Tom 17, Vypusk 2, Chast' 1
604 [Glaciers inventory of the USSR. Lena-Indigirka Basin, Chara and Vitim River Basins, (Kodar
605 Ridge)]. Vol. 17. Issue 2, Part 1, Gidrometeoizdat, Leningrad, 43 pp, in Russian, 1972.
- 606 Nuimura, T., Sakai, A., Taniguchi, K., Nagai, H., Lamsal, D., Tsutaki, S., Kozawa, A., Hoshina,
607 Y., Takenaka, S., Omiya, S., Tsunematsu, K., Tshering P., and Fujita K.: The GAMDAM glacier
608 inventory: a quality-controlled inventory of Asian glaciers, The Cryosphere, 9, 849-864, doi:
609 10.5194/tc-9-849-2015, 2015.
- 610 Osmonov, A., Bolch, T., Xi, C., Kurban A., and Guo W.: Glacier characteristics and changes in
611 the Sary-Jaz River Basin (Central Tien Shan, Kyrgyzstan) – 1990–2010, Remote Sensing
612 Letters, 4 (8), 725–734, doi:10.1080/2150704X.2013.789146, 2013.



- 613 Panagiotopoulos F., Shahgedanova M., Hannachi A., and Stephenson, D.B.: Observed Trends
614 and Teleconnections of the Siberian High: A Recently Declining Center of Action, *Journal of*
615 *Climate*, 18, 1411-1422, 2005.
- 616 Panagiotopoulos, F., Shahgedanova, M. and Stephenson, D.B.: A Review of Northern
617 Hemisphere Winter-time Teleconnection Patterns, *Journal of Physics France*, 12, 1027 – 1047,
618 2002.
- 619 Paul, F., Barry, R., Cogley, G., Frey, H., Haeberli, W., Ohmura, A., Ommanney, S., Raup, B.,
620 Rivera, A., and Zemp, M.: Recommendations for the compilation of glacier inventory data from
621 digital sources, *Annals of Glaciology*, 50 (53), 119-126, 2009.
- 622 Paul, F., Barrant, N.E., Baumann, S., Berthier, E., Bolch, T., Casey, K., Frey, H., Joshi, S.P.,
623 Konovalov, V., Le Bris, R., Mölg, N., Nosenko, G., Nuth, C., Pope, A., Racoviteanu, A.,
624 Rastner, P., Raup, B., Scharrer, K., Steffen, S., and Winsvold, S.: On the accuracy of glacier
625 outlines derived from remote-sensing data, *Annals of Glaciology*, 54 (63), 171-182, doi:
626 10.3189/2013AoG63A296, 2013.
- 627 Petrakov, D.A., Lavrent'yev, I.I., Kovalenko, N.V., and Usubaliev, R.A.: Tolshchina l'da, ob'em
628 i sovremennye izmeneniya ploshchadi lednika Sary-Tor (massiv Ak-Shyyrak, Vnutrenniy Tyan'-
629 Shan') (Ice thickness, volume and contemporary changes of the Sary-Tor glacier (Ak-Shiirak
630 Massive, Inner Tien Shan)). *Kriosfera Zemli (The Cryosphere of Earth)*, 18 (3), 91–100, in
631 Russian, 2014.
- 632 Pieczonka, T., Bolch, T., Junfeng, W., and Shiyin, L.: Heterogeneous mass loss of glaciers in the
633 Aksu-Tarim Catchment (Central Tien Shan) revealed by 1976 KH-9 Hexagon and 2009 SPOT-5
634 stereo imagery, *Remote Sensing of Environment*, 130, 233–244, doi:10.1016/j.rse.2012.11.020,
635 2013.
- 636 Pieczonka, T., and Bolch, T.: Region-wide glacier mass budgets and area changes for the Central
637 Tien Shan between ~1975 and 1999 using Hexagon KH-9 imagery, *Global and Planetary*
638 *Change*, 128, 1–13, doi: 10.1016/j.gloplacha.2014.11.014, 2015.



- 639 Puyu, W., Zhongqin, L., Wenbin, W., Huilin, L., Ping, Z., and Shuang, J.: Changes of six
640 selected glaciers in the Tomor region, Tian Shan, Central Asia, over the past ~50 years, using
641 high-resolution remote sensing images and field surveying, *Quaternary International*, 311, 123-
642 131, doi:10.1016/j.quaint.2013.04.031, 2013.
- 643 Racoviteanu, A.E., Williams, M.W., and Barry, R.G.: Optical Remote Sensing of Glacier
644 Characteristics: A Review with Focus on the Himalaya, *Sensors*, 8, 3355-3383, doi:
645 10.3390/s8053355, 2008.
- 646 Severskiy, I., Vilesov, E., Armstrong, R., Kokarev, A., Kogutenko, L., Usmanova, Z., Morozova,
647 V. and Raup, B.: Changes in glaciation of the Balkhash–Alakol basin, Central Asia, over recent
648 decades, *Annals of Glaciology*, 57 (71), 382- 394, doi: 10.3189/2016AoG71A575, 2016.
- 649 Shahgedanova, M., Nosenko, G., Khromova, T., and Muraveyev, A.: Glacier shrinkage and
650 climatic change in the Russian Altai from the mid-20th century: An assessment using remote
651 sensing and PRECIS regional climate model, *Journal of Geophysical Research*, 115, 1-12, doi:
652 10.1029/2009JD012976, 2010.
- 653 Shahgedanova, M., Nosenko, G., Kutuzov S., Rototaeva O., and Khromova T.: Deglaciation of
654 the Caucasus Mountains, Russia/Georgia, in the 21st century observed with ASTER satellite
655 imagery and aerial photography, *The Cryosphere*, 8, 2367-2379, doi:10.5194/tc-8-2367-2014,
656 2014.
- 657 Shangguan, D., Liu, S., Ding, Y., Ding, L., Xiong, L., Cai, D., Li, G., Lu, A., Zhang, S., and
658 Zhang, Y.: Monitoring the glacier changes in the Muztag Ata and Konggur mountains, east
659 Pamirs, based on Chinese Glacier Inventory and recent satellite imagery, *Annals of Glaciology*,
660 43, 79–85, 2006.
- 661 Shangguan, D., Liu, S., Ding, Y., Ding, L., Xu, J., and Jing L.: Glacier changes during the last
662 forty years in the Tarim Interior River basin, northwest China, *Progress in Natural Science*, 19,
663 727–732, doi:10.1016/j.pnsc.2008.11.002, 2009.



- 664 Shchetinnikov, A.S.: Morfologiya i rezhim lednikov Pamiro-Alaya (Morphology and regime of
665 the Pamir-Alai glaciers). Central Asia Hydro-Meteorological Institute, Tashkent, 219 pp., in
666 Russian, 1998.
- 667 Sneyers, R.: On the statistical analysis of series of observations. Tech. Note 143, WMO- 415,
668 192, 1990.
- 669 Solomina, O., Barry, R., and Bodnya, M.: The retreat of Tien Shan glaciers (Kyrgyzstan) since
670 the Little Ice Age estimated from aerial photographs, lichenometric and historical data,
671 *Geografiska Annaler*, 86 A (2), 205-215, 2004.
- 672 Sorg, A., Bolch, T., Stoffel, M., Solomina, O., and Beniston, M.: Climate change impacts on
673 glaciers and runoff in Tien Shan (Central Asia), *Nature Climate Change*, 2 (10), 725–731,
674 doi:10.1038/NClimate1592, 2012.
- 675 Stokes, C.R., Shahgedanova, M., Evans, I.S., and Popovnin, V.V.: Accelerated loss of alpine
676 glaciers in the Kodar Mountains, south-eastern Siberia, *Global and Planetary Change*, 101, 82-
677 96, doi:10.1016/j.gloplacha.2012.12.010, 2013.
- 678 Surazakov, A.B., and Aizen, V.B.: Positional accuracy evaluation of declassified Hexagon KH-9
679 mapping camera imagery, *Photogrammetric Engineering and Remote Sensing*, 76 (5), 603-608,
680 doi: 10.14358/PERS.76.5.603, 2010.
- 681 Vilesov, E. (ed.): Katalog Lednikov SSSR, Tsentral'nyy i Yuzhnyy Kazakhstan, Basseyn ozera
682 Balkhash, Basseyny rek Charyn, Tekes, Tom 13, Vypusk 2, Chast' 3, [Glaciers inventory of the
683 USSR. Central and Southern Kazakhstan, Balkhash lake Basin, Charyn and Tekes River Basins].
684 Vol. 13. Issue 2, Part 3, *Gidrometeoizdat*, Leningrad, 41 pp, in Russian, 1969.
- 685 Vilesov, E., Gorbunov, A., Morozova, V., and Severskiy, E.: Degradatsiya oledeneniya i
686 kriogenez na sovremennykh morenakh Severnogo Tyan'-Shanya, (Degradation of glaciation and
687 cryogenesis on the contemporary moraines of the northern Tien Shan). *Kriosfera Zemli* (The
688 Cryosphere of Earth), 10(1), 69–73, in Russian, 2006.



689 Wang P., Li, Zh., Li, H., Wang, W., Yao, H.: Comparison of glaciological and geodetic mass
690 balance at Urumqi Glacier No. 1, Tian Shan, Central Asia, *Global and Planetary Change*, 114,
691 14–22, doi:10.1016/j.gloplacha.2014.01.001, 2014.

692 Wang, L., Li, Z., Wang, F., Li., H., Wang, P.: Glacier changes from 1964 to 2004 in the Jinghe
693 River basin, Tien Shan, *Cold Regions Science and Technology*, 102, 78-83,
694 doi:10.1016/j.coldregions.2014.02.006, 2014.

695 Wang, L., Wang, F., Li, Z., Wang, W., Li., H., Wang, P.: Glacier changes in the Sikeshu River
696 basin, Tienshan Mountains, *Quaternary International*, 358, 153-159,
697 doi:10.1016/j.quaint.2014.12.028, 2015.

698 Wang, S., Zhang, M., Li, Z., Wang, F., Li, H., Li, Y., and Huang X.: Glacier area variation and
699 climate change in the Chinese Tianshan Mountains since 1960, *Journal of Geographical*
700 *Sciences*, 21(2), 263-273, doi: 10.1007/s11442-011-0843-8, 2011.

701 Wang, Y., Hou, S., Liu Y.: Glacier changes in the Karlik Shan, east ern Tien Shan, during
702 1971/72–2001/02, *Annals of Glaciology*, 50(53), 39-45, 2009.

703 Xu, JL.; Liu, SY.; Guo, WQ.; Zhang, Z.; Wei, JF.; and Feng, T.: Glacial Area Changes in the Ili
704 River Catchment (Northeastern Tian Shan) in Xinjiang, China, from the 1960s to 2009,
705 *Advances in Meteorology*, 1-12, doi:10.1155/2015/847257, 2015.

706
707
708
709
710
711
712
713
714



715 Table 1. Characteristics of temporal variability in temperature and precipitation time series from
 716 the Narynkol station. Values of R^2 referring to the linear trend in the time series significant at
 717 0.05 level are highlighted in bold. σ is standard deviation. Trends for precipitation are presented
 718 for two sub-periods because of the distinct opposite trends (Fig. 8).

Season	Temperature ($^{\circ}\text{C}$)			Precipitation (mm)					
	1947-2015			1952-1977			1977-2015		
	Mean $\pm\sigma$	$^{\circ}\text{C}/10 \text{ a}$	R^2	Mean $\pm\sigma$	mm a^{-1}	R^2	Mean $\pm\sigma$	mm a^{-1}	R^2
DJF	-10.8 \pm 1.6	+0.35	0.17	33 \pm 12	+0.3	0.03	36 \pm 10	+0.5	0.00
MAM	4.8 \pm 1.2	+0.27	0.19	113 \pm 36	-2.3	0.21	109 \pm 34	-0.3	0.01
JJA	15.2 \pm 0.7	+0.18	0.25	166 \pm 49	-3.9	0.33	158 \pm 38	+0.9	0.07
SON	4.2 \pm 1.3	+0.39	0.36	80 \pm 23	+0.3	0.01	84 \pm 30	+0.6	0.06
Annual	3.3 \pm 0.8	+0.30	0.54	393 \pm 78	-5.5	0.27	387 \pm 72	+1.3	0.04

719

720



721 Table 2. Details of the imagery used for glacier mapping.

Satellite	Sensor	Path/ row	Spatial resolution (m)	Acquisition date
Landsat 8	OLI TIRS	147r030	30 / 15 (panchromatic)	2013-09-09
Landsat 8	OLI TIRS	147r031	30 / 15 (panchromatic)	2013-09-09
Landsat 5	TM	147r030	30	1992-07-13
Landsat 5	TM	147r031	30	1992-07-13
KH-9 Hexagon			7.6	1976-01-12

722

723



724 Table 3. Area loss according to glacier size class.

Glacier size (km ²)	Number (1992)	Combined area (km ²)		Combined area change		Average area change	
		1992	2013	km ²	%	km ²	%
0.01 – 1.0	97	25.6±3.4	17.0±1.5	8.7±1.3	33.8±7.9	0.09±0.01	37.8±7.9
1 - 2	10	12.8±1.2	10.3±0.7	2.4±0.6	19.0±5.5	0.24±0.06	19.4±5.5
2 - 5	5	15.2±1.0	13.4±0.6	1.9±0.7	12.2±5.1	0.37±0.15	13.1±5.1
>5	6	67.8±3.7	64.3±2.7	3.4±3.3	5.1±5.1	0.57±0.56	6.8±5.1

725

726



727 Table 4. Area loss according to glacier type.

Glacier type	1992		1992	2013	Area reduction	
	No	Average size (km ²)	Area	Area	km ²	%
Compound - valley	3	16.3	48.7±2.6	46.9±1.9	1.85±2.4	3.8±5.1
Valley	21	2.2	45.6±3.2	39.0±2.0	6.53±2.2	14.3±5.8
Cirque-valley	19	0.62	11.7±1.2	8.9±0.6	2.82±0.6	24.1±6.1
Cirque	23	0.21	4.8±0.7	2.7±0.3	2.13±0.2	43.9±7.4
Hanging	49	0.19	9.3±1.3	7.1±0.6	2.25±0.5	24.1±9.0
Ice aprons	2	0.52	1.0±0.1	0.3±0.04	0.74±0.05	70.9±7.4
Flat-summit	1	0.2	0.2±0.03	0.1±0.01	0.08±0.01	47.6±6.5

728

729



730 Table 5. The combined area of 28 glaciers mapped using KH9 imagery (a) and its reduction (b)
731 between 1956 and 2013. Data for 1956 are from the Catalogue of Glaciers of the USSR (Vilesov
732 et al., 1969).

733 (a).

Year	1956	1976	1992	2013
Area, km ²	86,3	80,1±3,0	73,5±4,7	67,3±3,1

734

735 (b).

Period	Area reduction		
	km ²	%	
1956-1976	Total	6.2	7.14
	Per year	0.31	0.36
1976-1992	Total	6.7 ± 3.9	8.3 ± 5.6
	Per year	0.42 ± 0.24	0.52±0.35
1992-2013	Total	6.2 ± 3.6	8.4 ± 5.9
	Per year	0.30 ± 0.17	0.40±0.28
1976-2013	Total	12.9 ± 3.8	16.0 ± 5.8
	Per year	0.35±0.10	0.43±0.16
1956-2013	Total	19.0	22.0
	Per year	0.33	0.39

736

737



738 **Figure captions**

739 Figure 1. Study area.

740 Figure 2. Temperature (1947-2015) and precipitation (1952-2015) climatology for the Narynkol
741 station (Fig. 1).

742 Figure 3. An example of glacier outlines from (a) Landsat 8 OLI TIRS image from 2013 (black
743 outlines); (b) Landsat 5 TM image from 1992 (red outlines); and (c) Hexagon KH-9 image from
744 1976 (yellow outlines).

745 Figure 4. Area reduction according to glacier size (as in 1992).

746 Figure 5. Average rate of glacier area recession for different type of glaciers between 1992 and
747 2013.

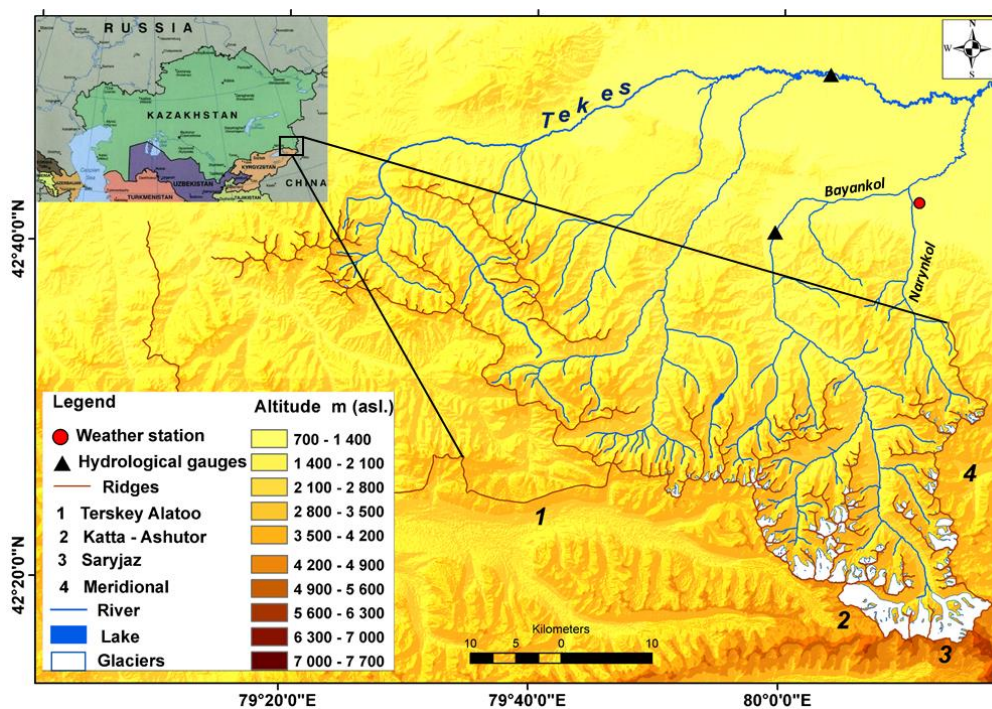
748 Figure 6. The combined area loss (a) (km²) and average rate of area loss (b) (% a⁻¹) by glaciers
749 with different aspects between 1992 and 2013.

750 Figure 7. Example of glacier changes between 1976 and 2013: Bayankol (91), Mramornaya
751 Stena (94) and Simonov (89). Landsat OLI TIRS image is used as background.

752 Figure 8. Seasonal temperature (°C) for the Narynkol station: (a) DJF; (b) MAM; (c) JJA; (d)
753 SON. The straight solid lines show record means. Note that different scales are used for different
754 seasons because of the large annual range.

755 Figure 9. Seasonal precipitation (mm) for the Narynkol station: (a) DJF; (b) MAM; (c) JJA; (d)
756 SON; (e) annual total. The straight solid lines show record means. Note that different scales are
757 used for different seasons because of the large annual range.

758 Figure 10. Comparison of glacier outlines derived in this study with glacier outlines presented in
759 RGI5.0 / GAMDAM (Nuimura et al., 2015). Higher-resolution SPOT imagery from 2007
760 illustrates the presence of crevasses in the accumulation zone of the Mramornaya Stena (No. 94)
761 glacier which confirm the presence of ice cover in the area excluded by RGI5.0 / GAMDAM
762 inventory.

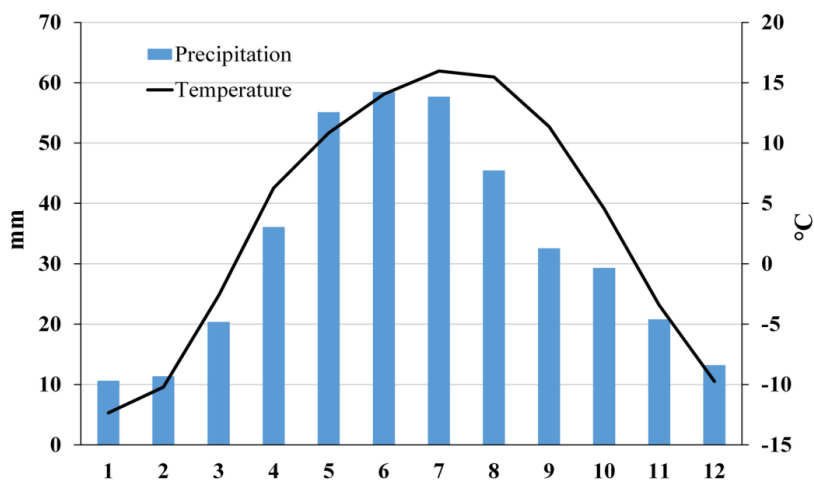


763

764

765 Figure 1. Study area.

766

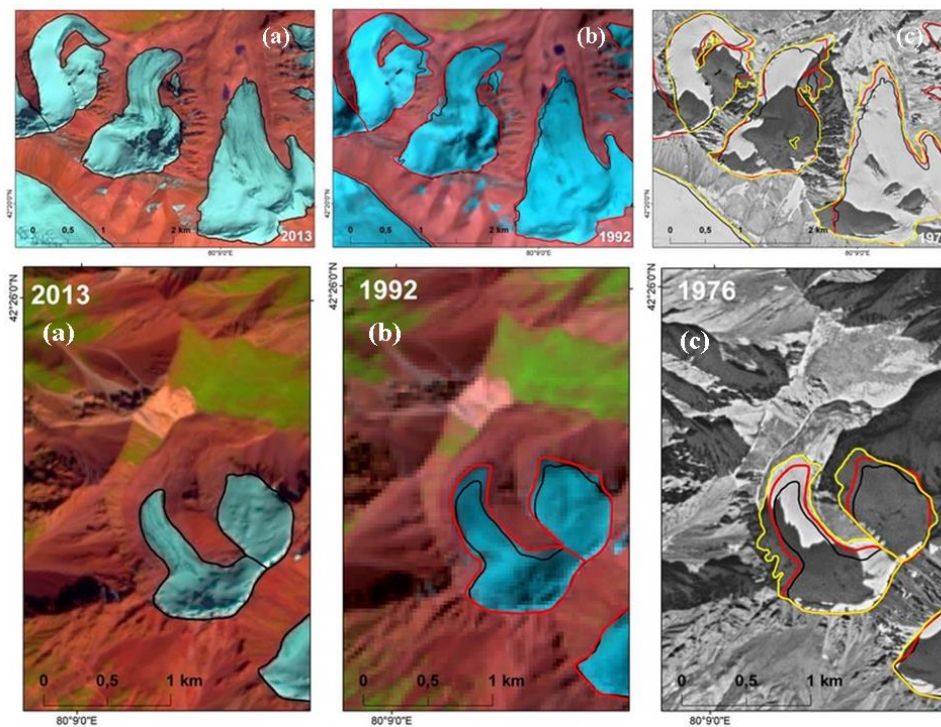


767

768

769 Figure 2. Temperature (1947-2015) and precipitation (1952-2015) climatology for the Narynkol
770 station (Fig. 1).

771

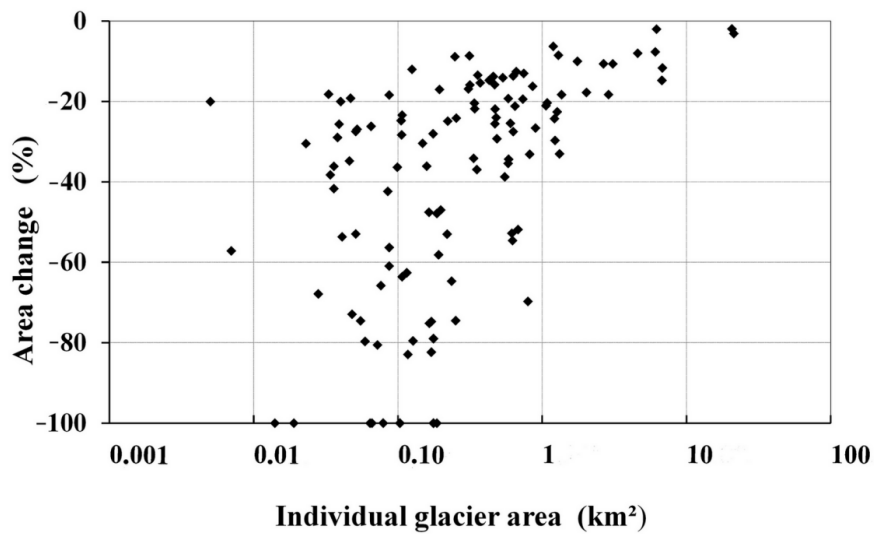


772

773

774 Figure 3. An example of glacier outlines from (a) Landsat 8 OLI TIRS image from 2013 (black
775 outlines); (b) Landsat 5 TM image from 1992 (red outlines); and (c) Hexagon KH-9 image from
776 1976 (yellow outlines).

777

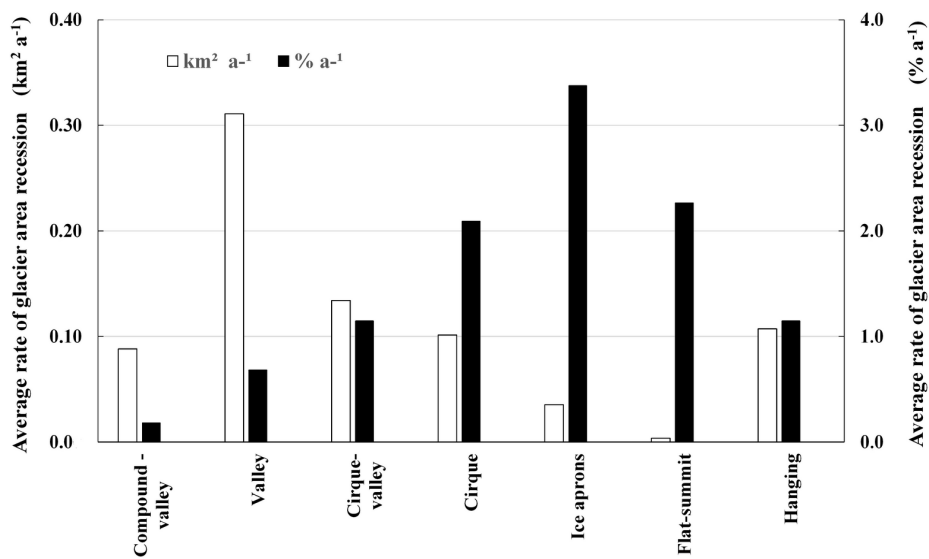


778

779

780 Figure 4. Area reduction according to glacier size (as in 1992).

781

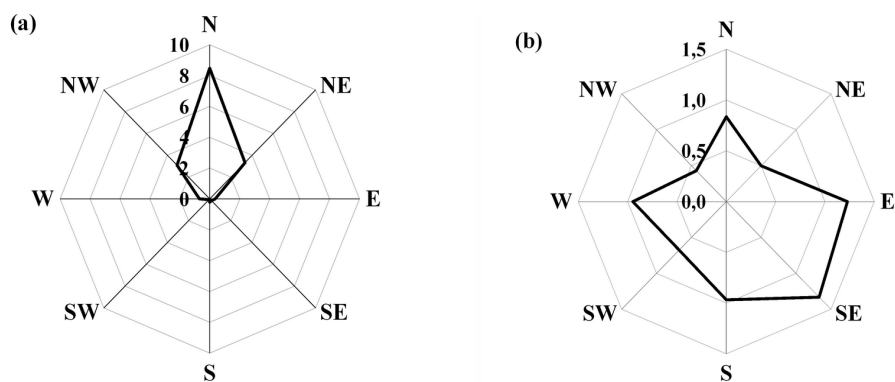


782

783

784 Figure 5. Average rate of glacier area recession for different type of glaciers between 1992 and
785 2013.

786

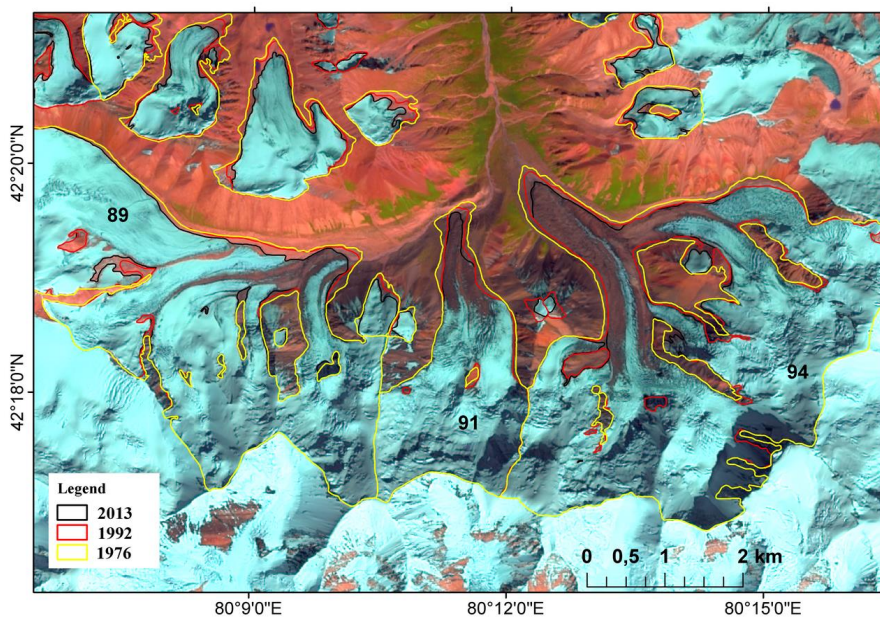


787

788

789 Figure 6. The combined area loss (a) (km²) and average rate of area loss (b) (% a⁻¹) by glaciers
790 with different aspects between 1992 and 2013.

791



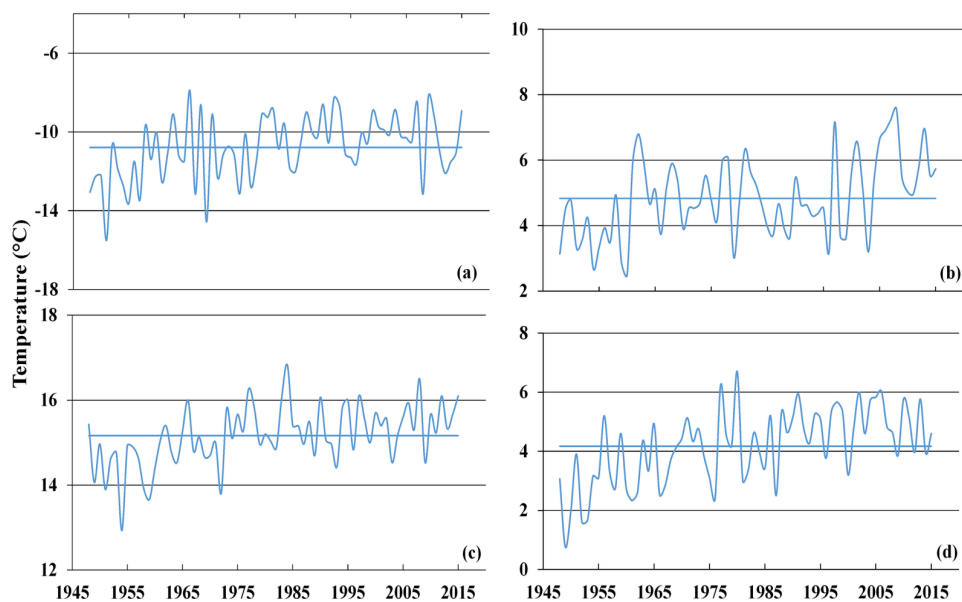
792

793

794 Figure 7. Example of glacier changes between 1976 and 2013: Bayankol (91), Mramornaya

795 Stena (94) and Simonov (89). Landsat OLI TIRS image is used as background.

796

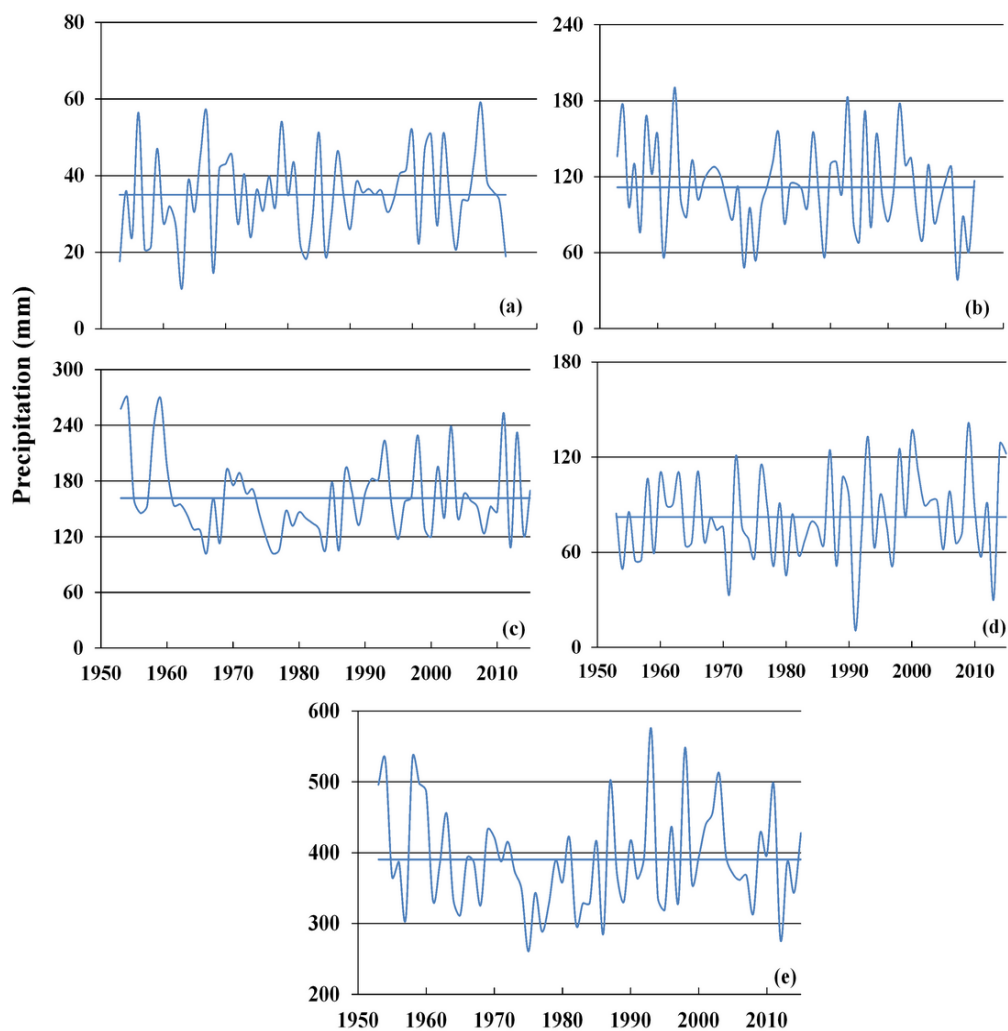


797

798

799 Figure 8. Seasonal temperature (°C) for the Narynkol station: (a) DJF; (b) MAM; (c) JJA; (d)
800 SON. The straight solid lines show record means. Note that different scales are used for different
801 seasons because of the large annual range.

802

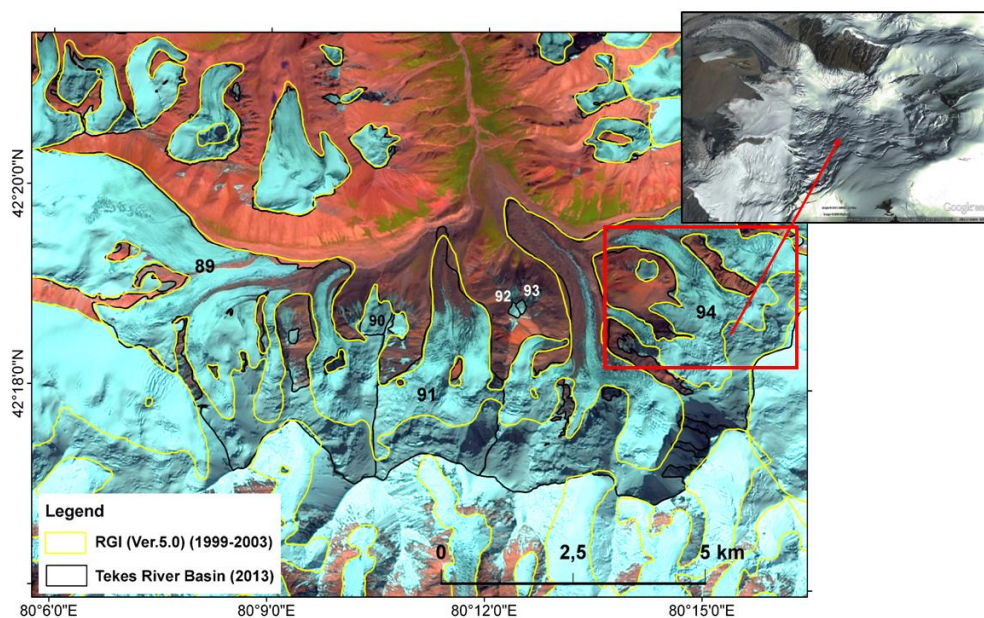


803

804

805 Figure 9. Seasonal precipitation (mm) for the Narynkol station: (a) DJF; (b) MAM; (c) JJA; (d)
806 SON; (e) Annual total. The straight solid lines show record means. Note that different scales are
807 used for different seasons because of the large annual range.

808



809

810

811 Figure 10. Comparison of glacier outlines derived in this study with glacier outlines presented in
812 RGI5.0 / GAMDAM (Nuimura et al., 2015). Higher-resolution SPOT imagery from 2007
813 illustrates the presence of crevasses in the accumulation zone of the Mramornaya Stena (No. 94)
814 glacier which confirm the presence of ice cover in the area excluded by RGI5.0 / GAMDAM
815 inventory.

816

817



818 Appendix A

819 Table A1. Results of assessments of glacier recession in Central Asia.

Region	Period	Number/area of investigated glaciers	Surface area reduction (%)	Reference
1	2	3	4	5
Northern Tien Shan				
Ala Archa basin	1963–2003	48/36.31 km ² in 2003	15.2	Aizen et al., 2006, 2007
	1963–1981	42.83 km ² in 1963	5.2	
	1981–2003	40.62 km ² in 1981	10.6	
Ala Archa Valley	1964-2010	40.9 ± 1.8 km ² in 1964	18.3 ± 5	Bolch, 2015
	1955-2008	307/287.3 km ² in 1955	41	
Northern slopes of Zailiyskiy Alatau				
	1955–1999	31/38.5 km ² in 1955	16.4	Bolch, 2007
Upper Chon-Kemin				
Chon-Aksu	1955–1999	48/62.8 km ² in 1955	38.2	
Sokoluk basin	1963–2000	77/31.7 km ² in 1963	28.0	
Niederer et al., 2007				
Ili River basin	1960s - 2007/2009	2119/2002.94 ± 152.2 km ² in 1960s	24.2 ± 8.8	Xu et al., 2015
Jinghe River basin	1964-2004	91/91.3 km ² in 1964	15.2	Wang et al., 2014
Sikeshu River basin	1964-2004	150/114.6 km ² in 1964	15.4	Wang et al., 2015
Central and Inner Tien Shan				
Akshirak Massif	1943-2003	178/371.6 km ² in 2003	12.5	Kuzmichenok, 1989; Aizen et al., 2006, 2007
	1977-2003	406.8 km ² in 1977	8.7	
	1943-1977	424.7 km ² in 1943	4.2	
Ak-shirak Range	1943-1977	more than 170/436 km ² in ~1950/60	3.0	Khromova et al., 2003, Khalsa et al., 2004
	1977-2001		20.0	
Ak-Shirak Massif	~1975 - ~2008	381 ± 15 km ² in ~1975	8.8 ± 4.8	Pieczonka and Bolch, 2015
KokShal-Too	~1975 - ~2008	587 ± 22 km ² in ~1975	1.6 ± 4.9	
Inylchek region	~1975 - ~2008	1074 ± 41 km ² in ~1975	3.0 ± 4.8	
Tomur region	~1975 - ~2008	964 ± 37 km ² in ~1975	2.5 ± 4.8	
Aksu Catchment	~1975 - ~2008	3539 ± 135 km ² in ~1975	3.6 ± 4.8	



1	2	3	4	5
Sary-Tor Glacier (Ak-Shyirak Massif)	1977-2003	1/3.54 km ² in 1977	0.77 % a ⁻¹	Petrakov et al., 2014, Aizen et al., 2007
	1987-2003		0.80 % a ⁻¹	
	2003-2012		0.67 % a ⁻¹	
Western Terskey Ala-Too	1971-2002	269/245 km ² in 1971	8.0	Narama et al., 2006
Eastern Terskey Ala-Too	LIA-2003	335/328 km ² in 2003	19.0	Kutuzov and Shahgedanova, 2009
	1965-2003	109/120 km ² in 1965	12.6	
	1990-2003	335/328 km ² in 2003	4.0	
Big Naryn basin	the mid 20th century - 2007	700/614,5 km ² in the mid-20 th century	23.4	Hagg et al., 2013
	the mid- 1970s-mid- 2000s	1478/1210 ±30 km ² in the mid-1970s	23.0	Kriegel et al., 2013
Pskem	1970-2000	525/219.8 km ² in ~1970	19	Narama et al., 2010
	2000-2007		5	
Ili-Kungöy	1970-2000	735/672.2 km ² in ~1970	12	
	2000-2007		4	
At-Bashy	1970-2000	192/113.6 km ² in ~1970	12	
	2000-2007		4	
SE-Fergana	1970-2000	306/190.1 km ² in ~1970	9	
	2000-2007		0	
Tarim Interior River basin	1960/70- 1999/2001	7665/17465.8 km ² in 1960/70	3.3	Shangguan et al., 2009
Qingbingtán Glacier No.72,	1964-2009	1/7.27 km ² in 1964	21.5	Puyu et al., 2013
Qingbingtán Glacier No.74,	1964-2009	1/9.55 km ² in 1964	14.7	
Keqikekuzibayi Glacier	1964-2007	1/25.77 km ² in 1964	6.8	
Tomor Glacier	1964-2009	1/310.14 km ² in 1964	0.3	
Qiongtailan Glacier	1964-2003	1/165.38 km ² in 1964	0.119 km ² a ⁻¹	
Sary-Jaz River Basin	1990-2010	1310/2055 ± 41.1 km ² in 1990	3.7 ± 2.7	Osmonov et al., 2013
Eastern Tien Shan				
Urumqi Glacier No. 1	1962-2009	2/1.646 km ² in 2009	16.0	P.Wang et al., 2014
Middle Chinese Tien Shan	1963-2000	70/48 km ² in 2000	13.0	Li et al., 2006



1	2	3	4	5
Mt. Bogda region	1962-2006	203/144.1 km ² in 1962	21.6	Li et al., 2011
Mt. Harlik region	1972-2005	75/98.3 km ² in 1972	10.5	
Mt. Karlik	1977-2013	156/136.84 km ² in 1977	21.9	Du et al., 2014
Karlik Shan	1971/72 - 2001/02	122/126 ± 1 km ² in 1971/72	5.3	Wang et al., 2009
Pamir				
Gissaro-Alay	1957–1980	4287/2183 km ² in 1957	15.6	Shchetinnikov, 1998
Pamir	1957–1980	7071/7361 km ² in 1957	10.5	
Pamiro-Alay	1957–1980	11358/9545 km ² in 1957	12.5	
Saukdara and Zulumart Ranges	1978–1990 1990–2001	5/33.7 km ² in 2001	7.8 11.6	Khromova et al., 2006
Muztag Ata and Konggur mountains	1962/66– 1999	302/835 km ² in 1962/66	7.9	Shangguan et al., 2006 Desinov and Kononov, 2007
Muksu River basin	1980–2000	-/468.4 km ² in 1980	7.4	Kononov, 2007
Muztagh Ata	1973-2013	-/274.3 ± 10.6 km ² in 1973	0.6 ± 3.9	Holzer, et al., 2015
Djungarskiy Alatau				
Southern Djungarskiy Alatau	1956–2011	460/228.4 km ² in 1956	47.4	Severskiy, I. et al., 2016
Northern Djungarskiy Alatau	1956–2012	343/294,6 km ² in 1956	38.4	
Western Djungarskiy Alatau	1956–2011	358/202.5 km ² in 1956	44.1	
Eastern Djungarskiy Alatau	1956–2012	208/88.4 km ² in 1956	42.9	Kaldybayev, et al., 2016
Karatal River basin	1956-2012	285/199.2 km ² in 1956	45.0	